Journal of Alloys and Compounds 504S (2010) S504–S507

Contents lists available at ScienceDirect

Journal of Alloys and Compounds

journal homepage: www.elsevier.com/locate/jallcom

Microstructure and thermoelectric properties of p-type Bi_2Te_3–Sb_2Te_3 alloys produced by rapid solidification and spark plasma sintering

ChulDong Moon[a,b], Sumin Shin[a], DoHyang Kim[b], Taek-Soo Kim[a,*]

[a] Dept. of Echo-materials and Processing, Korea Institute of Industrial Technology (KITECH), 7-47 Songdo-dong, Yeonsu-gu, Incheon 406-130, Republic of Korea
[b] Center for Non-crystalline Materials, Dept. of Advanced Materials Eng., Yonsei University, 134 Shinchon-dong, Seodaemun-gu, Seoul 120-749, Republic of Korea

ARTICLE INFO

Article history:
Received 4 August 2009
Received in revised form 12 March 2010
Accepted 15 March 2010
Available online 18 March 2010

Keywords:
Bi_2Te_3
Thermoelectric properties
Gas atomization
Spark plasma sintering (SPS)

ABSTRACT

P-type Te-doped Bi_2Te_3–Sb_2Te_3 compounds were prepared using rapid solidification and spark plasma sintering (SPS) techniques. The microstructure and thermoelectric properties were evaluated as a function of the SPS temperature. The phase distribution was characterized by X-ray diffraction (XRD) and examined by scanning electron microscope (SEM) and energy dispersive spectroscopy (EDS) area scanning. The thermoelectric properties were evaluated by a combination of thermal conductivity, electrical resistivity and Seebeck coefficient. The solidified powders consisted of homogeneous thermoelectric phase. As the SPS temperature increases, the microstructure become coarsen, resulting in the reduction of hardness. The thermoelectric figure of merit measured to be the maximum (3.05×10^{-3}/°C) at the SPS temperature of 430 °C.

1. Introduction

Bismuth telluride (Bi_2Te_3)-based alloys are known to present the most effective thermoelectric properties at the room temperature [1]. Although those have been widely produced using a type of unidirectional solidification process, powder metallurgy (PM) regards as a strong alternative in accordance with its merits conventionally known such as the high fabrication rate and the formation of fine microstructure and homogeneous phase distribution. In addition to the PM, combining the rapid solidification (RS) provides another opportunity of modifying the intrinsic brittleness and the thermoelectric anisotropy of the Bi–Te based thermoelectric materials [2]. The RS is good to suppress the peritectic reaction of the thermoelectric materials during the solidification, leading to the formation of thermoelectric phases bearing a stoichiometry of X_2Y_3 such as Bi_2Te_3, $Bi_2(TeSe)_3$ and $(BiSb)_2Te_3$ [3].

In this work, p-type materials were prepared using the gas atomization and Spark plasma sintering (SPS) processes. SPS is known to sinter the powder type materials at a relatively low temperature rapidly, since the pulsed current yielded during the SPS activated the powder surfaces in addition to its own joule heating [4]. The effect of the SPS processing parameter on the thermoelectric behavior of Te-doped Bi_2Te_3–Sb_2Te_3 was evaluated [5].

2. Experimental procedures

High purity (99.99%) Bi, Te and Sb granules were used to prepare the master alloy of 25% Bi_2Te_3 + 75% Sb_2Te_3 doped with 3 wt.% Te alloy. In order to fabricate the alloy powders, it was re-melted in a graphite crucible using the high frequency induction at the temperature of 200 °C above the liquidus temperature, bottom pouring through graphite melt delivery nozzle of 5 mm in diameter into a confined Ar gas atomizer operating at a pressure of 1.2 MPa [6,7]. The alloy powders under 90 μm selected using a conventional mechanical sieving technique were sintered using the spark plasma (SPSed) at different temperature of 330 °C, 380 °C, 430 °C, and 480 °C. Fig. 1 shows a schematic of SPS processing condition, in which the sample was heated up to 110 °C ($\sim X_1$) with the rate of 40 °C/min, holded for 10 min ($X_1 \sim X_2$) and then further heated with 60 °C/min ($X_2 \sim X_3$) followed by 5 °C/min ($X_3 \sim X_4$). Here, Y means each sintering temperature as 330 °C, 380 °C, 430 °C, and 480 °C, and $Y - 20$ means 20 °C below the each sintering temperature. The pressure applied during the SPS was about 50 MPa. For the microstructural analysis, scanning electron microscopy (SEM) (Model FEI-QUANTA 200F, USA) and energy dispersive spectroscopy (EDS) (Model EDAX Genesis, USA) were used. For the microstructural examination, the SPS samples were cut and etched using the agent of HNO_3:HCl (1:1). Grain size and the density were measured using the SEM and Archimedes method, respectively. The structures of both the powders as-atomized and the bulks SPSed were charcterized using XRD (Model D/Max 2500PC Rigaku, Japan).

The thermoelectric properties of the sintered Bi_2Te_3–Sb_2Te_3 bulks were measured at room temperature. The Seebeck coefficient (α) was determined using $\alpha = \Delta V/\Delta T$ with imposed temperature difference of 10 °C at both the ends of the specimen. The electrical resistivity (ρ) was measured using the four-probe technique. The thermal conductivity (κ) was measured by the static comparative method using transparent SiO_2 (κ = 1.36 W/m °C) as a standard sample in 5×10^{-5} Torr [8].

3. Results and discussion

XRD graph of powders (a) as-atomized and the bulks consolidated with the sintering temperature of (b) 330 °C, (c) 380 °C and

* Corresponding author. Tel.: +82 32 850 0409; fax: +82 32 850 0390.
E-mail address: tskim@kitech.re.kr (T.-S. Kim).

0925-8388/$ – see front matter © 2010 Published by Elsevier B.V.
doi:10.1016/j.jallcom.2010.03.114

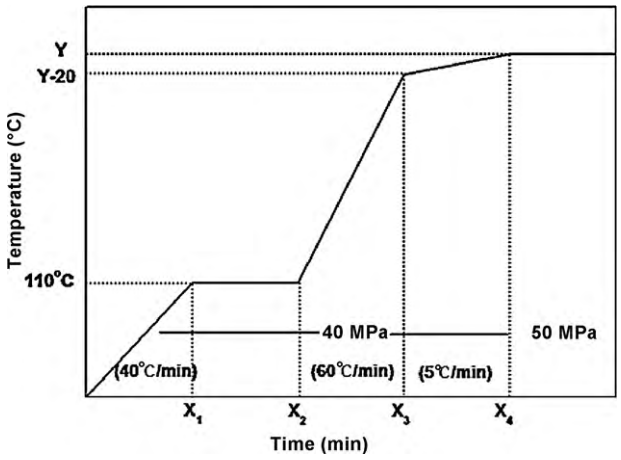

Fig. 1. Spark plasma sintering pattern of as-atomized Bi_2Te_3–Sb_2Te_3 powders.

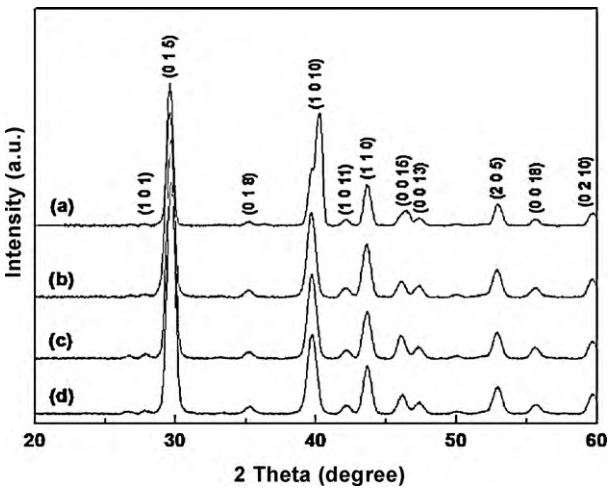

Fig. 2. XRD diffraction patterns of 25% Bi_2Te_3 + 75% Sb_2Te_3 doped with 3 wt.% Te alloys with (a) as-atomized and sintered temperature at (b) 330 °C, (c) 380 °C and (d) 430 °C.

Table 1
Compositions of p-type 25% Bi_2Te_3 + 75% Sb_2Te_3 alloys doped with 3 wt.% Te atomized and sintered.

	As-atomized	330 °C	380 °C	430 °C	480 °C
Bi	11.88	11.75	13.08	12.94	12.90
Te	59.63	59.56	58.50	57.89	57.67
Sb	28.47	28.65	28.39	29.11	29.32
Total	99.98	99.96	99.97	99.94	99.89

(d) 430 °C is shown in Fig. 2. It suggested that both the powders and the bulks only consisted of thermoelectric phases related with Bi_2Te_3–Sb_2Te_3. No particular change between the powders and sintered bulks in the peak position and intensity suggested that the phase and structure as solidified could be maintained even after the thermal sintering by SPS process.

According to the EDS data listed in Table 1, with increasing the sintering temperature from 330 °C to 380 °C, 430 °C and 480 °C, the quantity of Te gradually lowered from 59.56 to 58.50, 57.89 and 57.64, respectively. On the other hand, Bi and Sb, though their fluctuation showed somewhat opposite trend. This corresponds to the easy evaporation characteristic of Te compared to the other elements, which will lead the change of carrier concentration.

Fig. 3 shows the SEM microstructure of p-type Bi_2Te_3–Sb_2Te_3 bulks gas atomized and sintered with the temperature of (a) 330 °C, (b) 380 °C, (c) 430 °C and (d) 480 °C. It is seen that the alloy bar forms the needle type grains with various sizes, which is very typical for the alloys. The grain size increased from 5 μm to 20 μm as the SPS temperature increased from 330 °C to 480 °C, respectively. It is noted that the alloys formed the finer grains, compared to the grain sizes of 28–40 μm report by Hong and Chun, although both of them prepared by the gas atomization at the same condition [9]. This suggested that the combination of clean atomization and SPS is effective for forming and maintaining the fine grain size, respectively. The later may be due to the rapid sintering, corresponding to the pulsed current which conducts the powder surface activation and cleaning simultaneously. On the other hand, the former happened due to the rapid solidification, resulting in the suppression of coarsening the phases formed resulting from the rapid solidification.

Fig. 4 shows the variation of relative density and Vickers hardness of the sintered sample by SPS. The former gradually increased from 98.26% to 98.99%, 99.05% and 99.17% as the temperature increased from 330 °C to 380 °C, 430 °C and 480 °C, respectively. However, the micro-Vickers hardness tended to reduce with the temperature, being 64.32 Hv, 56.54 Hv, 53.58 Hv and 45.1 Hv, respectively. The highest value of 64.32 Hv (Fig. 4) at the lowest temperature of 330 °C is possibly due to the finest grain size, which is still higher than that obtained using the extrusion process [9].

Table 2 lists the value of Seebeck coefficient (α), electrical resistivity (ρ) and thermal conductivity (κ) of Bi_2Te_3–Sb_2Te_3 alloy bulks as a function of SPS temperature. Seebeck coefficient (α) is generally dependent on the scattering factor (γ) at a given temperature and the carrier concentration (n_c) as expressed as follows,

$$\alpha \approx \gamma - \ln\, n_c \quad (1)$$

Since the scattering occurs readily at the grain boundaries, α would be increased in the bulk sintered at the low temperature due to the existence of fine grains. The carrier concentration also became rich at the sample with the high sintering temperature, corresponding to the increase on the anti-defects by Te evaporation (Table 1). According to the Eq. (1), α became high at the low temperature range as well matched with Table 2. In addition, the decrease in the concentration and mobility of carrier with decreasing the temperature made the electric resistivity (ρ) high, in which the value (=0.94×10^{-5} Ωm) became the highest at the lowest temperature of 330 °C. On the other hand, at 480 °C, it was low to be 0.76×10^{-5} Ωm. Thermal conductivity showed a reverse behavior against the resistivity as shown in Table 2.

The figure of merit for the rapidly solidified and SPSed bulks at 330 °C, 380 °C, 430 °C and 480 °C was given at Table 2. The thermoelectric figure of merit was determined from the Seebeck cofficient (α), electrical resistivity (ρ) and thermal conductivity (κ), as given by $Z = \alpha^2/\rho\kappa$ [10–12]. The Z value became maximum of 3.05×10^{-3}/°C at 430 °C, which is higher than 2.79×10^{-3}/°C mea-

Table 2
Seebeck coefficient (α), electrical resistivity (ρ), thermal conductivity (κ) and figure of merit (Z) sintered temperature at 330 °C, 380 °C, 430 °C and 480 °C.

	Seebeck coefficient (uV/°C)	Electrical resistivity (10^{-5} Ωm)	Thermal conductivity (W/m °C)	Figure of merit ($\times 10^{-3}$/°C)
330 °C	180.22	0.94	1.30	2.65
380 °C	187.53	0.93	1.33	2.84
430 °C	180.81	0.81	1.32	3.05
480 °C	176.98	0.76	1.45	2.84

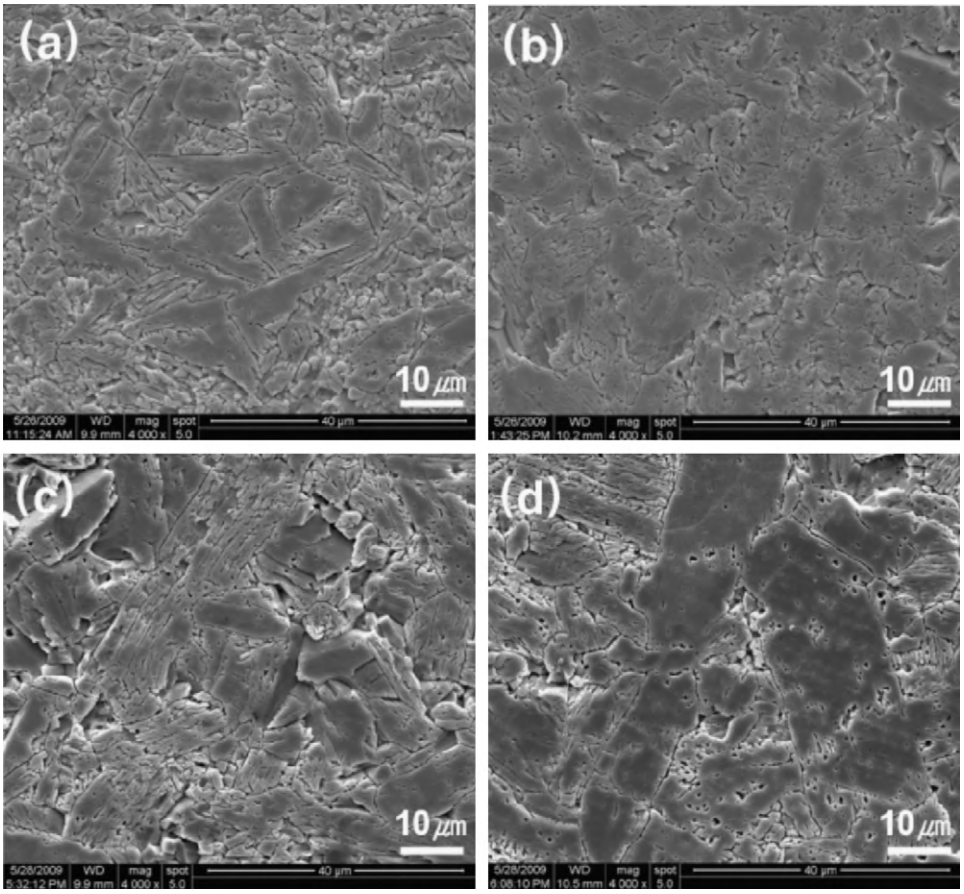

Fig. 3. Scanning electron micrographs showing the surface of spark plasma sintering (SPS) at (a) 330 °C, (b) 380 °C, (c) 430 °C and (d) 480 °C.

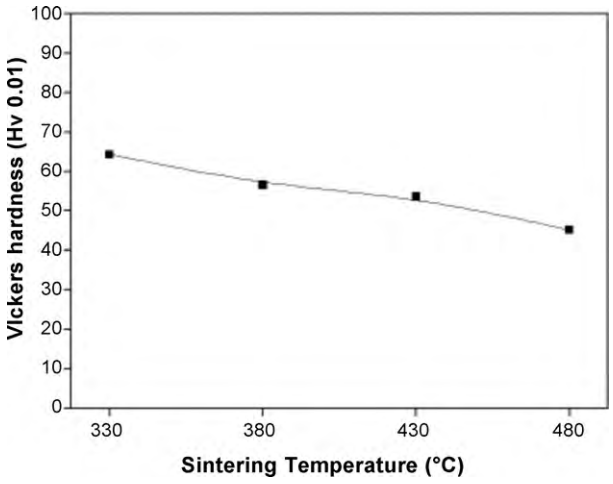

Fig. 4. The micro-Vickers hardness of spark plasma sintering with variety sintered temperature.

sured from the sample prepared by the same composition and PM process and annealing effect alloys of about [13]. This result may correspond to the decrease of form an excellent sintered body powders.

4. Conclusion

Rapidly solidified p-type Bi_2Te_3–Sb_2Te_3 alloy doped with Te powders were synthesized using the gas atomization, followed by SPS. The sample rapidly solidified and spark plasma sintered formed a thermoelectric phases. Increasing the SPS temperature induced a reduction in the hardness from 64.3 Hv to 45.1 Hv due to the coarsening of the grains. The figure of merit of SPSed bulks was varied from 2.65×10^{-3}/°C, 2.83×10^{-3}/°C, 3.05×10^{-3}/°C and 2.84×10^{-3}/°C, respectively. Combination of closed gas atomization and SPS process resulted in processing the high quality thermoelectric specimen due to the rapid and low temperature sintering of the powders. The variation in attributted to the change of Seebeck coefficient, electric resistivity and thermal conductivity, which is of consistent of Z and, also varied mainly with the grain size and the carrier concentration.

Acknowledgement

This research was supported by a grant from Ministry of Knowledge Economy (MKE) of the Industrial core technology development, Republic of Korea.

References

[1] D.J. Yeon, T.S. Oh, D.-B. Hyun, H.W. Lee, J. Korean Inst. Met. Mater. 38 (1) (2000) 159.
[2] T.-S. Kim, B.-S. Chun, J. Alloys Compd. 437 (2007) 225.
[3] T.-S. Kim, I.-S. Kim, T.-K. Kim, S.-J. Hong, B.-S. Chun, Mater. Sci. Eng. B90 (2002) 42.
[4] I.-S. Kim, C.-W. Hwang, D.-K. Paik, J. Korean Inst. Met. Mater. 36 (4) (1998) 597.
[5] D.-B. Hyun, H.-P. Ha, J.-S. Hwang, T.-S. Oh, J. Korean Inst. Met. Mater. 38 (1) (2000) 153.
[6] S.-J. Hong, S.-H. Lee, B.-S. Chun, Mater. Sci. Eng. B98 (2003) 232.
[7] K.H. Lee, J.H. Park, B.S. Chun, J. Korean Inst. Met. Mater. 43 (8) (2005) 553.

[8] C.H. Lim, K.T. Kim, Y.H. Lee, C.H. Lee, D.C. Cho, C.H. Lee, Intermetallics 14 (2006) 1370.
[9] S.-J. Hong, B.-S. Chun, Mater. Res. Bull. 38 (2003) 599.
[10] S.-J. Hong, Y.-S. Lee, J.-W. Byeon, B.-S. Chun, J. Alloys Compd. 414 (2006) 146.
[11] J.-S. Lee, H.-C. Kim, D.-B. Hyun, T.-S. Oh, J. Korean Inst. Met. Mater. 37 (5) (1999) 609.
[12] J.S. Hwang, D.B. Hyun, T.S. Oh, H.W. Lee, J.D. Shin, J. Korean Inst. Met. Mater. 36 (4) (1998) 601.
[13] T.-S. Kim, B.S. Chun, J.K. Lee, H.G. Jung, J. Alloys Compd. 434–435 (2007) 710.